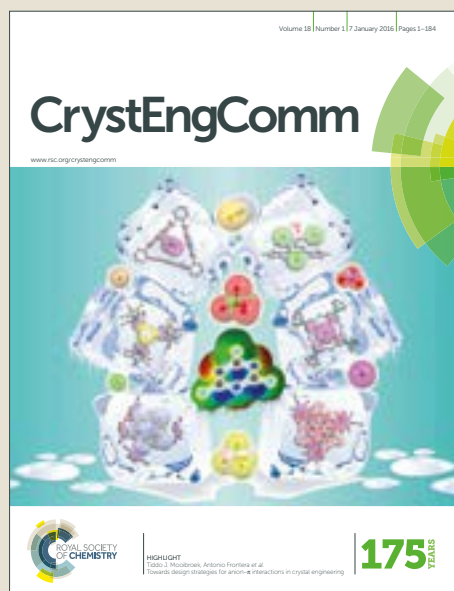


CrystEngComm

Accepted Manuscript



This is an Accepted Manuscript, which has been through the Royal Society of Chemistry peer review process and has been accepted for publication.

Accepted Manuscripts are published online shortly after acceptance, before technical editing, formatting and proof reading. Using this free service, authors can make their results available to the community, in citable form, before we publish the edited article. We will replace this Accepted Manuscript with the edited and formatted Advance Article as soon as it is available.

You can find more information about Accepted Manuscripts in the [author guidelines](#).

Please note that technical editing may introduce minor changes to the text and/or graphics, which may alter content. The journal's standard [Terms & Conditions](#) and the ethical guidelines, outlined in our [author and reviewer resource centre](#), still apply. In no event shall the Royal Society of Chemistry be held responsible for any errors or omissions in this Accepted Manuscript or any consequences arising from the use of any information it contains.



Received 00th January 20xx,

New insights into polymer mediated formation of anatase mesocrystals

Olga V. Boytsova,^{*abc} Alexey A. Sadovnikov,^b Khursand E. Yorov,^c Artemii N. Beltiukov,^d Alexander E. Baranchikov,^b Vladimir K. Ivanov,^{b,e} Xiangli Zhong,^f David J. Lewis,^f Paul O'Brien^{f,g} and Andrew J. Sutherland^{*a}

Accepted 00th January 20xx

DOI: 10.1039/x0xx00000x

www.rsc.org/

The reaction between $(\text{NH}_4)_2\text{TiF}_6$ and H_3BO_3 in the presence of varying quantities of PEG-6000 was used to form NH_4TiOF_3 mesocrystals (MCs). The amount of PEG-6000, employed as a template, is crucial to the formation of defect free, non-agglomerated NH_4TiOF_3 MCs; high concentrations lead to MC agglomeration, lower ones result in centralized defects. This polymer-mediated formation process may be understood using an analogy with known polymerization reactions. The oxofluorotitanate MCs readily undergo a thermal topotactic transformation to give anatase MCs with photocatalytic activity. The TiO_2 MCs are porous, with highly orientated lamellar crystallites that form part of the larger mesocrystal structure.

Introduction

Mesocrystals^{1,2} are a relatively new class of materials with potential in many applications³⁻⁵ which were first defined by Cölfen.⁶ They are ordered assemblies (superstructures) of individual single crystals, each of which often have critical dimensions of the order of nanometres. Such structures are common in nature⁷ and chemists have developed routes to, and some models of, MC formation; polymers are often used to facilitate the formation of the aggregate.^{6,8,9} The shape, period, size and morphology of the self-organized structures (MCs) show a strong structural dependence upon the polymer used. Such structures may be important for: photocatalysis,^{10,11} dye-sensitized solar cells,¹¹ fibre optics,⁶ sensors,⁶ and bioimplants.¹²

Following the original work on the polymer-mediated growth of anatase using Brij polymers,^{13,14} many groups have

reported on this methodology for the synthesis of such materials.^{15,17} Typically the mesocrystals formed are flat lozenges with truncated corners. The underlying crystal structure can be used to understand aspects of the origin of this shape. The unit cell of anatase is shown in Fig. 1. It is a tetragonal crystal and the conventional unit cell is shown in Fig 1a. One way to view this structure is as two interpenetrating tetragonal lattices one for Ti with 2 titanium atoms and 6 vacancies, the second of O atoms with 4 oxygens and 4 vacancies, with the atoms in the positions defined for forming a unit cell Fig. 1b. The unit cell with Ti at (0,0,0) is also shown in Fig. 1c, with the tetragonal points for the Ti lattice shown. A recurring unit is also found at edge lengths of $a/2$ and $c/2$ with 16 lattice points across two sub-lattices. However, the cell can be further simplified to the asymmetric unit Fig 1b.

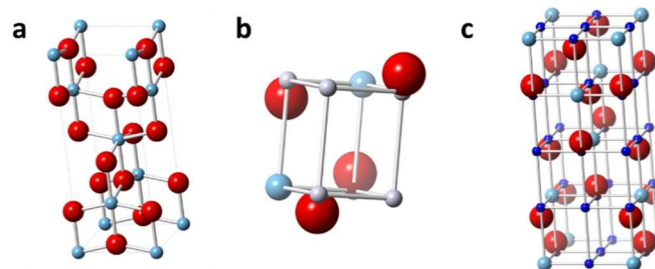


Fig. 1. Unit cells and the construction of anatase. **a)** The conventional unit cell $a = 3.785 \text{ \AA}$, $c = 9.514 \text{ \AA}$ ³¹ **b)** The structure is built from atom complete asymmetric units, the origin of the lattice can be either on Ti or O but Ti is normally chosen. There are two special positions (0,0,0 and 0,0,2081). The tetragonal lattice can be based on either atom in combination with vacancies. These lattice points are shown in **b)** and **c)** which is again the unit cell. The relationship to the cubic derived tetragonal symmetry is clear in **c)** but somewhat disguised in the conventional representation **a)**.

^a Aston Institute of Materials Research, Aston University, Birmingham, B4 7ET, UK. E-mail: o.boytsova@aston.ac.uk, a.j.sutherland@aston.ac.uk

^b Kurnakov Institute of Inorganic Chemistry of RAS, Moscow, Russia, 119991, Leninskii Ave. 31.

^c Lomonosov Moscow State University, Moscow, Russia, 119992, Leninskii Gory, 1.

^d Physical-Technical Institute of UB RAS, Izhevsk, 426000 Russia, Kirova str. 132

^e Tomsk State University, Tomsk, Russia, 634050, Lenina av.36

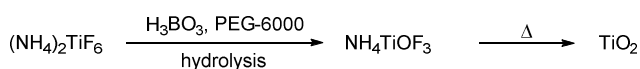
^f School of Materials, University of Manchester, Oxford Road, Manchester, M13 9PL, UK.

^g School of Chemistry, University of Manchester, Oxford Road, Manchester, M13 9PL, UK.

Electronic Supplementary Information (ESI) available: [Materials and Experimental procedures, SEM and TEM micrographs, XRD and SAED patterns, Raman spectrum, FT-IR spectra, TGA analysis and MC size distribution data]. See DOI: 10.1039/x0xx00000x

This approach which we have used earlier¹⁸ can be powerful in analysing small crystals and their faceting. The unit can also be thought of as comprising $\text{Ti}_2\text{O}_4\text{Y}_2$ where all points are associated with the Ti tetragonal lattice with Y representing a vacancy in that lattice and O a pairing of a vacancy and an oxygen atom. An important feature of such units is that they are stoichiometric and hence can in imagination be made from real atoms, for any number or replications of the unit whilst maintaining both charge balance and stoichiometry.

In this work we have generated mesocrystals of anatase from PEG-6000 templated MCs of ammonium oxofluorotitanate, NH_4TiOF_3 . These were prepared using an aqueous mixture of $(\text{NH}_4)_2\text{TiF}_6$ and H_3BO_3 in the presence of PEG-6000 as a promoter/template.¹⁷ Subsequently, the thermal, topotactic conversion to anatase TiO_2 can be easily achieved (Scheme 1).¹⁷



Scheme 1. Equation showing the chemical reactions involved in the formation of both NH_4TiOF_3 and TiO_2 MCs from the titanium-containing precursor $(\text{NH}_4)_2\text{TiF}_6$.

In pioneering work, Stucky^{19,20} and Yang *et al.*²¹ had suggested in the formation of TiO_2 -containing films, generated at interfaces, that a ratio of $(\text{NH}_4)_2\text{TiF}_6 : \text{H}_3\text{BO}_3$ of 1:2 is optimal for the generation of anatase.^{22,23} A later study but the first to form mesocrystalline TiO_2 used Brij@58 (an amphiphilic block copolymer, $\text{C}_{16}\text{H}_{33}(\text{OCH}_2\text{CH}_2)_{20}\text{OH}$) and showed that varying the polymer concentration had an effect on MC formation.¹⁵

In this work we have generated NH_4TiOF_3 MCs using PEG 6000. A model to describe this process has been developed which enables rationalisation of the effects of the PEG on MC morphology. It is important to note that the actual control of crystal growth is in the formation of NH_4TiOF_3 precursor as its morphology is essentially fully retained during subsequent thermal topotactic transformation of NH_4TiOF_3 MCs into TiO_2 MCs, and in turn directly relates to the photocatalytic properties of the TiO_2 MCs.

Experimental section

Reagents were sourced from the suppliers indicated and were used as received. $(\text{NH}_4)_2\text{TiF}_6$ (Sigma-Aldrich UK) 0.1 mol L⁻¹ poly(ethylene glycol) PEG-6000 (Alfa Chemicals Ltd.) and gelation agent H_3BO_3 (Alfa Chemicals Ltd.) 0.2 mol L⁻¹ were dissolved in distilled water (30 mL) under continuous stirring. After full dissolution of the reagents, the resultant gel was kept at 35 °C for 20 hours. The resultant precipitate was isolated by centrifugation/decantation and subsequently washed with water (3 x 20 mL) and acetone (3 x 20 mL). In the present work four different PEG-6000 to $(\text{NH}_4)_2\text{TiF}_6$ to H_3BO_3 molar ratios were used (0:4:8, 1:4:8, 1:2:4 and 3:4:8). The results obtained in this system are similar to those reported for Brij systems previously.¹⁷ Samples of NH_4TiOF_3 MCs (ca. 0.5 g) were heated in air at 450 °C for 2, 4 or 8 hours. A Nabertherm HTCT 03/14

furnace was used and exhaust gases were vented into a fume cupboard.

X-Ray Diffraction (XRD) was conducted on a Bruker D8 Advance system using monochromatic $\text{CuK}\alpha$ radiation. SEM was performed on a Carl Zeiss NVision 40 electron microscope. TEM was performed on a FEI Tecnai G2 F30 electron microscope with resolution of 0.14 nm. Raman spectroscopy was conducted using a Renishaw inVia Reflex spectrometer with an illumination wavelength of 633 nm.

Thermogravimetric analysis was carried out using a Perkin-Elmer Thermogravimetric Analyzer Pyris 1. Heating was conducted from room temperature to 800 °C with a heating rate increase of 5 °C / min. BET Low temperature nitrogen adsorption measurements were conducted using an ATX-6 analyzer (Katakona, Russia). Before measurements the samples (30–60 mg weight) were outgassed at 200 °C for 30 min under a dry helium flow.

Determination of the surface area was carried out by the 5-point Brunauer, Emmett and Teller (BET) method at the relative pressure range of $P/P_0 = 0.05 - 0.25$.

Measurements of photocatalytic activity were conducted under irradiation of a suspension of the analyte MC with an Ocean Optics HPX- 2000 deuterium-halogen lamp (the output power is 1.52 mW, as measured in the 200–1100 nm range by an integrated optical power meter) in a cell thermostated at 37 °C. Spectrophotometric analysis was performed using an Ocean Optics QE65000 spectrometer. All samples were kept in the dark for 45 minutes prior to conducting the degradation study.

Results and discussion

Mesocrystals of NH_4TiOF_3 were prepared in gels and separated as described in the experimental section. Samples of TiO_2 MCs, were formed by annealing NH_4TiOF_3 at 450 °C in air, for 2, 4 or 8 h, and then analysed by XPS (Fig. 2). Table 1 summarizes these results which show that the C/Ti ratio reduces with time to 0.39, at greater than 4 h of annealing. This observation confirms that the high temperature annealing causes loss of a significant amount of carbonaceous materials, from PEG-6000, in line with its decomposition profile which is generally held to involve the loss of short oligomers.^{24,25}

Table 1 Atomic concentration of components of MCs from XPS

Sample	Ti	O	C	F	K	C/Ti	F/Ti
NH_4TiOF_3 MCs	11.88	23.32	12.45	41.7	0.75	1.05	3.5
TiO_2 MCs (2 h anneal)	20.72	53.54	11.65	8.98	5.11	0.56	0.43
TiO_2 MCs (4 h anneal)	21.71	54.87	8.40	10.37	4.65	0.39	0.48
TiO_2 MCs (8 h anneal)	21.60	55.87	8.47	9.33	4.73	0.39	0.43

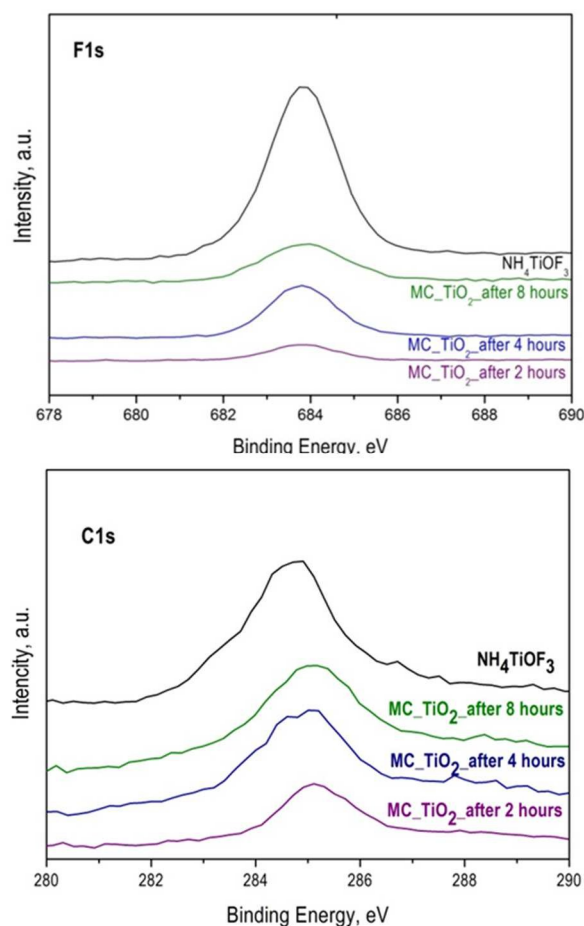


Fig. 2 XPS spectra of the F 1s region and C 1s of NH_4TiOF_3 and samples of MC TiO_2 MCs, formed by annealing NH_4TiOF_3 at 450°C after heating for 2 hours (purple line), 4 hours (blue line) and 8 hours (green line).

Much of the fluoride is also lost as the conversion from NH_4TiOF_3 MCs to TiO_2 MCs proceeds, although some fluoride remains even after extended heating. This XPS data, in conjunction with the structural data (*vide infra*), indicates that the optimal duration of annealing at 450°C is around 4 hours. Between 4 and 8 hours there is little change in the XPS data but after 8 hours the mesocrystalline superstructure of the TiO_2 MCs starts to break down

Our rather complete analysis gives considerable insight into the material formed and several interesting observations can be made. Potassium persists in the final materials presumably a contaminant from the PEG. The carbon analysis enables stoichiometries, before and after various heating periods, to be determined (Fig. 3) and in particular to permit the number of PEG units per titanium to be estimated. The elemental analysis suggests that there are ca 247 titanium atoms per PEG polymer. We know that the lattice parameters are very similar in the precursor and anatase phases,⁸ and that in the toptactic process we lose fluoride from and gain an

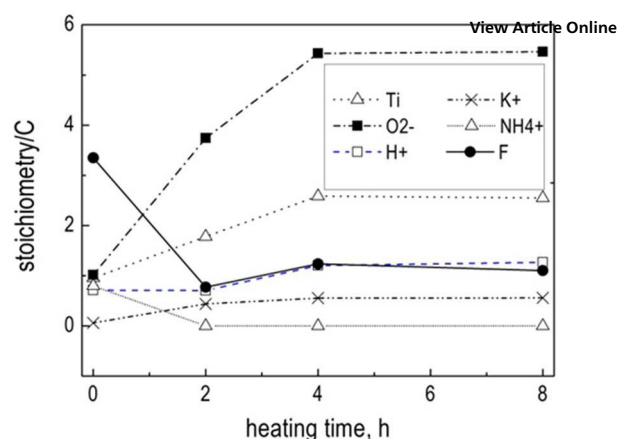


Fig. 3. XPS-derived elemental stoichiometries present in the NH_4TiOF_3 mesocrystals ($t=0$) and TiO_2 mesocrystals formed by annealing NH_4TiOF_3 at 450°C for 2, 4 and 8 hours.

oxide ion to the TiO_x lattice. In the (001) plane the Ti atoms sit in a simple square lattice separated by 3.784 \AA , the unit cell is very similar in x and y in NH_4TiOF_3 .⁸ The only plane available for the bonding of the PEG or related modifier is this (001) type. It is easy from this information to calculate the number of Ti atoms per PEG on a surface of the precursor. This analysis suggests that there are around 256 titanium atoms per PEG 6000 (based on the RMM of PEG and the ratio of titanium and carbon atoms in the salt). It is reasonable to make the assumption that this arrangement might form a single nano crystallite. This unit would be defined by a 16×16 square of titanium atoms each at a separation of 3.745 \AA , or a ca 6 nm square. It may not be a coincidence that the PEG 6000 polymer contains about 133 oxygens that could bind to titanium and that a random walk on this square lattice might be expected to cover 50% of such sites very close to $256/2$. In addition an energy minimised conformation of PEG suggests a separation of ca 2.7 \AA between adjacent oxygens on the polymer backbone, remarkably close to the Ti Ti separation. The typical form of the mesocrystal is shown in Fig. 4.

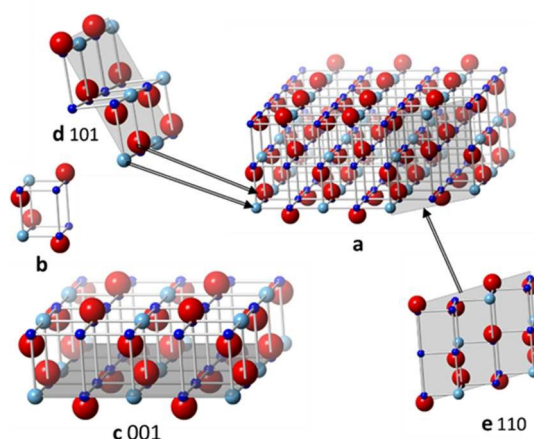


Fig. 4 shows a model of the mesocrystal a) and its building block b). The second most stable face (001) is dominant c) hence growth is inhibited in the z direction. The normally dominant (101) face d) is not seen. However the corners of the crystals are most often cut along (110) see a) and e). All these more stable faces are neutral using closely adjacent atoms and can be built from the asymmetric unit b).

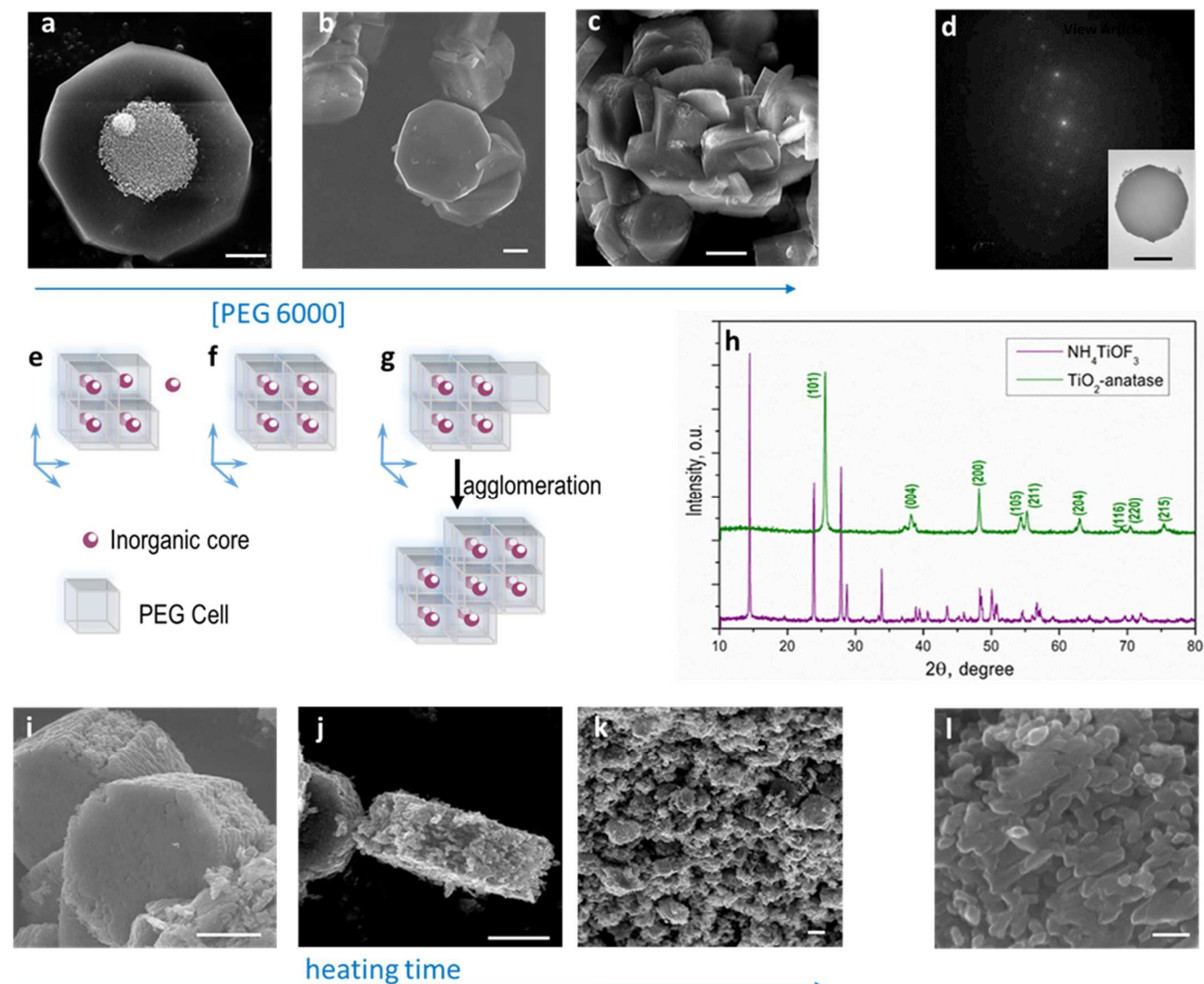


Fig. 5 SEM micrographs of NH_4TiOF_3 MCs formed from $(\text{NH}_4)_2\text{TiF}_6$ and H_3BO_3 from in the presence of a) too little PEG-6000 (PEG-6000 : $4(\text{NH}_4)_2\text{TiF}_6$: $8\text{H}_3\text{BO}_3$), b) close to the optimal amount of PEG-6000 (PEG-6000 : $2(\text{NH}_4)_2\text{TiF}_6$: $4\text{H}_3\text{BO}_3$), and c) too much PEG-6000 (3PEG-6000 : $4(\text{NH}_4)_2\text{TiF}_6$: $8\text{H}_3\text{BO}_3$); d) SAED pattern for the NH_4TiOF_3 MC sample as shown in the inset TEM image; Schematic representation of the process of NH_4TiOF_3 MCs formation from $(\text{NH}_4)_2\text{TiF}_6$ and H_3BO_3 in the presence of e) too little PEG-6000 (PEG-6000 : $4(\text{NH}_4)_2\text{TiF}_6$: $8\text{H}_3\text{BO}_3$), f) close to the optimal amount of PEG-6000 (PEG-6000 : $2(\text{NH}_4)_2\text{TiF}_6$: $4\text{H}_3\text{BO}_3$), and g) too much PEG-6000 (3PEG-6000 : $4(\text{NH}_4)_2\text{TiF}_6$: $8\text{H}_3\text{BO}_3$); h) Representative XRD patterns from NH_4TiOF_3 MCs (lower line) and TiO_2 MCs (upper line). SEM images of TiO_2 MCs formed by the thermal topotactic transformation of the NH_4TiOF_3 MCs shown in b) after heating at 450°C for i) 2 hours, j) 4 hours and k) 8 hours; l) Magnified SEM micrograph of the TiO_2 MCs shown in Fig 5i) (NB the white scale bars in the bottom right of each SEM micrograph = $1\ \mu\text{m}$, except Fig 5l where it = $100\ \text{nm}$, the black scale bar in 5(d) = $2\ \mu\text{m}$).

It is important to remember that the crucial event is the formation of NH_4TiOF_3 which has only two Ti faces for coordination, in a crystal, and it is on this that the shape of the anatase mesocrystal depends. The fact that anatase mesocrystals are formed with some (110) facets possibly suggests that the Ti rich equivalent face equivalent surface in the precursor also appears. This effect may be associated with some PEG binding to this face at higher concentrations.

Whilst all NH_4TiOF_3 MCs formed retained the same overall shape, size and thickness (Table 2), at the lower PEG-6000 ratios (1:4:8) MCs with an outer crystalline region and an inner region potentially comprising nanocrystallites of TiO_2 ¹⁵ (Fig. 5a) formed. Conversely too much PEG-6000 (i.e. 3:4:8) resulted in agglomerated crystals (Fig. 5c) with surface defects and even

central holes (ESI). At closer to the optimal amount of PEG (i.e. 1:2:4) smooth, regular and uniformly-sized NH_4TiOF_3 MCs were formed (Fig. 5b).

Once uniform NH_4TiOF_3 MCs had been obtained they were heated and the topotactic transformation into anatase occurred.^{8, 10} Annealing times of 2, 4 or 8 hours were used and the resultant materials characterized by SEM, FT-IR, Raman and XRD and the TiO_2 MCs were assessed for their photocatalytic efficiency.

In the 2-D system devised by Moriguchi *et al*²³ NH_4TiOF_3 was grown at an air/water monolayer of dioctadecyldimethylammonium bromide. The surfactant monolayer was believed to serve as a 2-dimensional template for the oriented growth of crystalline NH_4TiOF_3 .²³ PEG and

Table 2 Summary of the size and properties of the various mesocrystals and nanocrystals formed from $(\text{NH}_4)_2\text{TiF}_6$ and H_3BO_3 (in the optimal PEG-6000 : $(\text{NH}_4)_2\text{TiF}_6$: H_3BO_3 1:2:4 molar ratio) followed by annealing at 450°C for the times shown.

Property	MCs NH_4TiOF_3 (0 h anneal)	MCs TiO_2 (2 h anneal)	MCs TiO_2 (4 h anneal)	Nano- crystals TiO_2 (8 h anneal)
Geometric size*, μm	2.0-2.5	2.0-2.5	2.0-2.5	-
Thickness*, μm	0.8-1.1	0.8-1.3	0.8-1.5	-
Edge Angle*, °	38.9	54.07	28.96	N/A
BET, m^2/g	1 ± 0.1	20 ± 2.0	19 ± 1.9	7 ± 0.7
Photodegradation, %/min	-	0.06	0.11	0.03

* See ESI for definition of dimension measurements

other polymers may serve a similar role to an air/water interface. In the present system, the substrate is likely to self-assemble in 3-dimensions^{26,27} rather than two. MC formation occurs in an environment in which crystallization is initiated in an aqueous 'gel-like' environment bounded by PEG-6000. In this case a fixed amount of $(\text{NH}_4)_2\text{TiF}_6$ and H_3BO_3 (in a molar ratio of 1:2) will generate a fixed number of initiation sites in a given volume of PEG. The fixed $(\text{NH}_4)_2\text{TiF}_6$ and H_3BO_3 ratio also ensures that the amount of fluoride released (varying concentrations of fluoride are known to affect the MC morphology¹¹) is also kept constant. This conceptualization of the preliminary crystallization process enables a prediction to be made of the outcome of too much or too little PEG-6000 in the mixture that is consistent with a previous study which showed correlation between the amount of added Brij and MC morphology.²⁶

This model is analogous to controlled polymerization reactions, such as RAFT²⁸ and ATRP,²⁹ from which a narrow size distribution of nascent polymers results. Control over the dispersity index in these systems is achieved by the generation of a defined number of initiation sites which subsequently all grow at the same rate as the monomer is consumed. An equal growth rate is achieved due to the fact that the propagating radicals are in rapid equilibrium with a dormant species and thus the propagating radicals are present only in small amounts relative to the dormant species.^{28,29} Similarly, in the case of MCs, if an appropriate amount of PEG-6000 is present the number of nucleation sites fits nicely the volume of 3-dimensional matrix formed by the PEG, a situation as shown schematically (Fig. 5f). Nucleation then leads to oriented crystal growth which generates a crystallographically aligned cluster of nanocrystallites all initiated at roughly the same time and all growing at a similar rate until the precursors, within the polymer-bounded matrix are exhausted.

If too little PEG-6000 is present there is an excess of $(\text{NH}_4)_2\text{TiF}_6$ present over the number of polymer-based nucleation sites (Fig. 5e). This results in an additional process of crystallization, leading to the formation of a characteristic central region within the NH_4TiOF_3 MCs. In this region, previous studies have shown that NH_4TiOF_3 is not the main

species present, since there is an excess of titanium relative to fluoride, consistent with the direct formation of TiO_2 .¹⁵ Conversely excess PEG-6000 (Fig. 5g) triggers reaction between similar units, in analogy to the formation of mineral bridges described by Stucky in the formation of abalone nacre or pearl,⁷ Fig. 5g. This hypothesis allows prediction of the effect of varying individual components. For example, too little boric acid would reduce the volume of the PEG-bounded region and so should result in MC formation with characteristic abnormalities at the centre of the crystal as shown in Fig. 5a. If too much boric acid is present the volume of reactive media is too great for the number of nucleation sites and so agglomeration (Fig. 5c) would be predicted. These ideas agree with the findings from a previous study, where the effect of varying the amount of boric acid was studied.⁸

It is important to note that the model is empirical since it does not in a simple way rely on a fixed molar volume of the PEG. The situation is more complex than that since it is known that the hydrophilicity/hydrophobicity, and indeed the solution phase size of PEG polymers is significantly affected by the external environment.³⁰ Boric acid is likely to change the nature of the PEG environment modifying its properties and molecular volume and hence the influence it exerts upon MC formation.

To further establish that this model is applicable to other systems, the MCs in the current study were characterized to verify that they do not differ significantly from $(\text{NH}_4)_2\text{TiOF}_3$ MCs generated from systems such as the Brij-based one.¹⁵ The SEM images (Fig. 5i-5l) provides clear evidence of the size and morphology of the TiO_2 MCs, formed by annealing NH_4TiOF_3 at 450°C (Fig. 3(l) and ESI). The images show clearly how the MC's surface morphology is transformed upon annealing. The smooth surfaces of the parent NH_4TiOF_3 MCs become roughened and appear to be considerably more porous. The longer the annealing time, the smaller the volume of the resulting TiO_2 MCs. The decrease in volume is consistent with the conversion process involving the loss of water, HF and the decomposition of PEG-6000. The surface area of the resultant material initially increases with increased annealing times, as observed by BET analysis (Table 2). Extended heating times (8 hours) gave a form that broke down to give a powder presumably because the organic polymer ligands between the nanocrystallites decompose. Interestingly, breakdown of the mesocrystalline superstructure caused by this extended heating, resulted in the surface area being reduced significantly (Fig. 5k, Table 2)

The XRD (Fig 5h) of both the NH_4TiOF_3 and TiO_2 MCs gave the following cell parameters; NH_4TiOF_3 $a = 7.552 \text{ \AA}$, $b = 7.583 \text{ \AA}$, $c = 12.630 \text{ \AA}$ (cf^{26} $a = 7.5594 \text{ \AA}$, $b = 7.5754 \text{ \AA}$, $c = 12.7548 \text{ \AA}$)²⁶ and TiO_2 $a = 3.793 \text{ \AA}$, $c = 9.485 \text{ \AA}$ (cf^{31} $a = 3.785 \text{ \AA}$, $c = 9.514 \text{ \AA}$) Thermal treatment gave rise to well-oriented assemblies of anatase TiO_2 single aligned nanoparticles, which have apparent average sizes of between several and tens of nanometers. The p-XRD pattern of the TiO_2 formed after 2, 4 and 8 hours of thermal treatment are very close to the cell parameters of anatase (ESI) The TiO_2 MC nanocrystals, formed after 8 hours of annealing, have slightly increased peak intensities in the

XRD. The SAED patterns confirm orientation within the matrix of the NH_4TiOF_3 MCs (Fig. 5d, ESI). Thermogravimetric analysis (TGA) gave profiles similar to those reported previously for the conversion of Brij-templated NH_4TiOF_3 MCs into TiO_2 MCs.²⁶ Four distinct steps were observed (ESI).²⁶

Analysis of the TiO_2 MCs by Raman spectroscopy confirmed anatase TiO_2 (ESI), FT-IR spectroscopy (ESI) also confirmed that both MC formation steps had proceeded successfully. Specifically, for NH_4TiOF_3 MCs the appearance of a signal at 720cm^{-1} corresponds to the combination of the lattice modes of Ti-O and Ti-F and a signal at 920cm^{-1} is consistent with the stretching mode of Ti=O or the asymmetric Ti-O-Ti stretching.^{14,32,33}

Subsequent loss of NH_4^+ in conversion of NH_4TiOF_3 MCs into TiO_2 MCs is also evidenced by a complete loss of modes at 3274 , 3184 and 3075cm^{-1} and a dramatic reduction in the N-H bending frequency at 1410cm^{-1} .^{34,35} The p-XRD data, enabled the estimation of nanocrystallite size by using the Scherrer equation giving crystalline dimensions of the ab plane of TiO_2 of ca. 30-35 nm which is in reasonably good agreement with the size determined by SEM (ESI).

Previously the presence of F adsorbates on TiO_2 has been reported to enhance photocatalytic activity.³⁶⁻³⁹ The origin of this effect has been ascribed to both the fluoride promoting enhanced free hydroxyl radical production³⁶ but also and perhaps more importantly helping to promote formation of/stabilise the most photocatalytically reactive (001) facets.³⁷⁻³⁹ Moreover reconstruction of the surface can occur which can also enhance photocatalytic activity. Thus to establish if PEG-6000 favours formation of photocatalytically reactive species, the three types of TiO_2 MCs were assessed for their photocatalytic efficiency directly without any further modification. Each TiO_2 MC sample was incubated with an aqueous solution of crystal violet and the resultant solution exposed to UV light.^{10,40} Decreasing dye intensity over time gives a measure of photocatalytic efficiency (ESI). As a control experiment NH_4TiOF_3 MCs were also similarly assessed and showed no evidence of dye degradation. The greatest photocatalytic efficiency was observed for TiO_2 MCs formed after a 4 hour anneal. Two hours produced MCs with reasonable activity, however annealing for 8 hours reduced efficiency. The relationship between photocatalytic efficiency and annealing time likely reflects loss of active (001) facets together with reduction in the accessible surface. The surface areas values and the efficiencies of the three different TiO_2 MCs, together with their various properties and those of the parent NH_4TiOF_3 MCs are shown in Table 2.

Conclusions

The polymer, PEG-6000, can serve as an effective template for NH_4TiOF_3 MCs formation. Variation of the amount of PEG-6000 shows an optimum molar ratio of PEG-6000 to $(\text{NH}_4)_2\text{TiF}_6$ to H_3BO_3 of 1:2:4. The reagent ratio gave rise to smooth, regular and uniformly-sized NH_4TiOF_3 MCs which in turn can be converted thermally into anatase. Optimization of this process resulted in anatase TiO_2 MCs with good photocatalytic

efficiencies which are comparable with data reported elsewhere for such systems.¹⁰

The work has also given new insights into the formation of anatase mesocrystals and in particular sheds light on how the Ti-PEG interactions serve to direct the crystallisation process. Determining the ratio of Ti atoms to PEG enabled a model to be developed for the MC formation process. Although only empirical, this model allows for the effect of PEG-6000 concentration on the resultant MC morphology to be rationalized. These ideas fit well with previous studies.^{1,2,4,5} Although TiO_2 is prone to form well faceted anatase crystals PEG-6000 clearly affects the final overall morphology. Moreover, the photocatalytic activity observed for the TiO_2 MCs indicates the polymer does promote 001 facet formation. Since morphology is critical for MC properties, such as photocatalytic activity, careful identification of the optimal polymer additive and concentration must be used to prevent classical crystallisation taking over. Work to this effect is ongoing in our laboratories.

Acknowledgements

We acknowledge the support of the European Commission (Grant PolyCOMP no. 661317), the Russian Foundation of Basic Research (project # 15-38-70045) and RF President Grant (MK-336.2017.3)

Notes and references

- H. Cölfen and M. Antonietti, *Angew. Chem. Int. Ed.*, 2005, **44**, 5576.
- E. V. Sturm and H. Cölfen, *Chem. Soc. Rev.*, 2016, **45**, 5821.
- V. K. Ivanov, P. P. Fedorov, A. Y. Baranchikov and, V. V. Osiko, *Russ Chem Rev*, 2014, **83**, 1204.
- L. Zhou and P. O'Brien, *Small*, 2008, **4**, 1566.
- L. Zhou and P. O'Brien, *J. Phys. Chem. Lett.*, 2012, **3**, 620.
- H. Cölfen and S. Mann, *Angew. Chem. Int. Ed.*, 2003, **42**, 2350.
- C. Zaremba, A. M. Belcher, M. Fritz, Y. Li, S. Mann, P. K. Hansma, D. E. Morse, J. S. Speck and G. D. Stucky, *Chem. Mater.*, 1996, **8**, 679.
- L. D. Zhou, D. Smyth-Boyle and P. O'Brien, *J. Am. Chem. Soc.* 2008, **130**, 1309.
- R.-Q. Song and H. Cölfen, *Adv. Mater.*, 2010, **22**, 1301.
- L. Zhou, J. Chen, C. Ji, L. Zhou and P. O'Brien, *CrystEngComm.*, 2013, **15**, 5012.
- X. Fu, C. Fan, S. Yu, L. Shi and Z. Wang, *J. Alloy Compd.*, 2016, **680**, 80-86.
- N. A. J. M. Sommerdijk and G. de With, *Chem. Rev.*, 2008, **108**, 4499.
- J. Feng, M. Yin, Z. Wang, S. Yan, L. Wan, Z. Li and Z. Zou, *CrystEngComm.*, 2010, **12**, 3425.
- L. Zhou, D. S. Boyle and P. O'Brien, *Chem. Commun.*, 2007, 144.
- Y. Liu, Y. Zhang, H. Tan and J. Wang, *Cryst. Growth Des.*, 2011, **11**, 2905.
- Y. Liu, Y. Zhang, H. Li and J. Wang, *Cryst. Growth Des.*, 2012, **12**, 2625.
- M. Inoguchi, M. Afzaal, N. Tanaka and P. O'Brien, *J. Mater. Chem.*, 2012, **22**, 25123.
- P. J. Thomas and P. O'Brien, *J. Am. Chem. Soc.*, **128**, 5614.

- 19 P. Yang, D. Zhao, D.I. Margolese, B. F. Chmelka and G. D. Stucky, *Nature*, 1998, **396**, 152-155.
- 20 J. Tang, Y. Wu, E. W. McFarland and G. D. Stucky, *Chem Commun.*, 2004, 1670.
- 21 H. G. Yang, C. H. Sun, S. Z. Qiao, J. Zou, G. Liu, S. C. Smith, H. M. Cheng and G. Q. Lu, *Nature*, 2008, **453**, 638.
- 22 S. Deki, Y. Aoi, Y. Asaoka, A. Kajinami and M. Mizuhata, *J. Mater. Chem.*, 1997, **7**, 733.
- 23 I. Moriguchi, K. Sonoda, K. Matsuo, S. Kagawa and Y. Teraoka, *Chem. Commun.*, 2001, 1344.
- 24 K. J. Voorhees, S. F. Baugh and D. N. Stevenson, *Therm. Chim Acta*, 1996, **274** 187.
- 25 K. J. Voorhees, S. F. Baugh and D. N. Stevenson, *J. Anal. Appl. Pyrolysis*, 1994, **30**, 47.
- 26 L. Zhou and P. O'Brien, *Phys. Status Solidi A.*, 2008, **205**, 2317.
- 27 L. Y. Shteinberg, *Russ. J. Appl. Chem.*, 2009, **82**, 613.
- 28 G. Moad, E. Rizzardo and S. H. Thang, *Polymer*. 2008, **49** 1079.
- 29 T. Pintauer and K. Matyjaszewski, *Chem. Soc. Rev.*, 2008, **37**, 1087.
- 30 H. Kawamura, M. Manabe and K. Miyake, *Langmuir*, 1995, **11**, 1653.
- 31 R. W. G. Wyckoff *Crystal Structures*, Second edition; Interscience Publishers, New York, USA, 1963, **1**, 239-444.
- 32 N. M. Laptash, I. G. Maslennikova and T. A. Kaidalova, *J. Fluor. Chem.* 1999, **99**, 133.
- 33 J. Okuda and E. Herdtweck, *Inorg. Chem.*, 1991, **30**, 1516.
- 34 H. Stuart, *Infrared Spectroscopy: Fundamentals and Applications*; John Wiley & Sons Ltd: New York, USA, 2004, pp 96-97.
- 35 H. B. Wu, M. N. Chan and C. K. Chan, *Aerosol Sci. Technol.*, 2007, **41**, 581.
- 36 K. Lv and Y. Xu *J. Phys. Chem. B*, 2006, **110**, 6204.
- 37 A. Selloni, *Nat. Mater.*, 2008, **7**, 613.
- 38 H. G. Yang, C. H. Sun, S. Z. Qiao, J. Zou, G. Liu, S. C. Smith, H. M. Cheng and G. Q. Lu, *Nature*, 2008, **453**, 638.
- 39 J. Pan, G. Liu, G. Q. Lu and H.-M. Cheng, *Angew. Chem. Int. Ed.*, 2011, **50**, 2133.
- 40 A. A. Sadovnikov, A. E. Baranchikov, Y. V. Zubavichus, O. S. Ivanova, V. Y. Murzin, V. V. Kozik and V. K. Ivanov, *J. Photochem. Photobiol A: Chem.*, 2015, **303-304**, 36.

[View Article Online](#)

Title: "New insights into polymer mediated formation of anatase mesocrystals"

New details of the non-classical formation of TiO_2 mesocrystals (MCs) from NH_4TiOF_3 MCs are described

Authors: Olga V. Boytsova, Alexey A. Sadovnikov, Khursand E. Yorov, Artemii N. Beltiukov, Alexander E. Baranchikov, Vladimir K. Ivanov, Xiangli Zhong, David J. Lewis, Paul. O'Brien and Andrew J. Sutherland

